A Flash Photolysis Resonance Fluorescence Investigation of the Reaction $OH + H_2O_2 \rightarrow HO_2 + H_2O$

MICHAEL J. KURYLO, JENNIFER L. MURPHY, GEOFFREY S. HALLER, and KENNETH D. CORNETT

Chemical Kinetics Division, Center for Chemical Physics, National Bureau of Standards, Washington, DC 20234

Abstract

The flash photolysis resonance fluorescence technique has been used to measure the rate constant for the reaction

$$OH + H_2O_2 \xrightarrow{k_1} HO_2 + H_2O$$

over the temperature range of 250–370 K. The present results are in excellent agreement with three very recent studies, and the combined data set can been used to derive the expression

$$k_1 = (2.91 \pm 0.30) \times 10^{-12} \exp[-(161 \pm 32)/T] \text{ cm}^3/\text{molecule s}$$

similar to that currently used in atmospheric modeling applications.

A summary of our computer simulation of this reaction system is presented. The results of the computations indicate the absence of secondary reaction complications in the present work while revealing significant problems in the earlier (pre-1980) studies of the title reaction.

Introduction

The role of HO_x chemistry in the earth's atmosphere has been well documented by both laboratory and computer simulations [1]. In the troposphere such species serve to initiate hydrocarbon oxidation, while in the stratosphere they catalytically destroy ozone as well as participate in the interconnection of reaction cycles involving NO_x, ClO_x, and other catalysts. Hydrogen peroxide serves as an important atmospheric reservoir for HO_x, the OH/HO_2 ratio being influenced both by title reaction (1) and H_2O_2 photolysis:

(1) $$OH + H_2O_2 \rightarrow HO_2 + H_2O$$

(2) $$H_2O_2 + h\nu \rightarrow OH + OH$$

The H_2O_2 itself is generated primarily by hydroperoxyl radical combination:

International Journal of Chemical Kinetics, Vol. 14, 1149–1161 (1982)
 CCC 0538-8066/82/101149-13$02.30

(3) $$HO_2 + HO_2 \rightarrow H_2O_2 + O_2$$

a reaction whose temperature dependence appears quite complex [2]. This complexity, coupled with the lack of direct observation of stratospheric H_2O_2, results in moderate uncertainty in the species' atmospheric importance. In addition, the sequence of reaction (1) followed by reaction (3) is equivalent to reaction (4), which exerts a controlling influence on stratospheric HO_x concentrations [3,4]:

(4) $$OH + HO_2 \rightarrow H_2O + O_2$$

The role of reactions (1) plus (3) as an HO_x sink is strongest in the troposphere and lower stratosphere, where calculated H_2O_2 concentrations are greatest. Thus a quantitative assessment of this cycle requires accurate representation of k_1 under atmospheric conditions. Similarly, a knowledge of k_1 and its temperature dependence is necessary when reaction (1) is used as an HO_2 source in laboratory studies and/or is present as a reference reaction in such investigations. For example, measurements of the rate constants for the reactions of HO_2 with both OH and O have required knowledge of k_1.[1]

Earlier absolute measurements [6–8] of k_1 yielded room temperature values ranging from 6.8 to 9.3×10^{-13} cm^3/molecule s, while two relative rate studies [9,10] resulted in k_1 values of 6.2×10^{-13} and 12×10^{-13} cm^3/molecule s, respectively. The agreement between two absolute temperature dependence determinations [6,7] gave rise to a recommended rate expression [11] of $k_1 = 1.0 \times 10^{-11} \exp(-750/T)$ cm^3/molecule s despite the fact that the preexponential factor seemed unreasonably high for an abstraction reaction of this type. However, two recent reinvestigations of reaction (1) [12,13] by discharge-flow resonance fluorescence present a markedly different picture of the atmospheric importance of reaction (1) than drawn by the earlier measurements. The new k_1 values range from a factor of 2 larger at room temperature to more than three times greater at stratospheric temperatures, thereby placing reaction (1) on a more competitive basis with H_2O_2 atmospheric photolysis. Due to the significance of these changes in k_1 we felt that a confirmation of the new discharge flow results under significantly different experimental conditions would be desirable, providing such additional work could explain the sources of disagreement with the earlier studies. Since the two recent flow investigations attributed these differences to secondary chemistry, we have attempted to quantify this appraisal based on the results of our own flash photolysis resonance fluorescence (FPRF) investigation and detailed modeling computations. During the course of our experiments we became aware of an ongoing laser photolysis resonance fluorescence study, the results of which are now published [14] and confirm the recent flow results.

[1] This dependence on k_1 is discussed for the individual reactions in [5].

While the confirmatory aspect of our investigation is now lessened, we feel that a quantitative description of our modeling exercise is instructive in demonstrating the role of competing secondary reactions in various concentration regions as well as in defining sources of judgment or analysis error in the various experimental techniques. This latter point is important both in the evaluation of other kinetic studies and in the conduct of future experiments.

Experimental

The apparatus used in this study has been detailed in a very recent publication [15]. Briefly, the experiments were performed with a spherical, all Pyrex, double-walled reaction cell (~100 cm^3 volume). OH radicals were produced by the flash photolysis of reactant mixtures consisting of H_2O_2 (0–20 mtorr), H_2O (~100 mtorr), and Ar (20, 30 torr). The N_2 pulsed-discharge flash lamp used for this purpose was equipped with quartz optics, and the OH thus produced was detected in real time using the previously described resonance fluorescence procedures [16]. Data acquisition and mathematical analysis of the decay curves were as outlined in our earlier studies [17].

The reaction mixtures in more concentrated form were prepared manometrically in 10-L glass storage bulbs prior to their being metered through the reaction cell (~100 cm^3/s) at pressure between 20 and 30 torr [1 torr = 133.32 Pa = $9.6587 \times 10^{18}/T(K)$ molecule cm^3]. This flow procedure minimizes significant depletion of H_2O_2 by reaction, photolysis, or heterogeneous decomposition. The magnitude of k_1 restricted the use of H_2O_2 partial pressures to below 20 mtorr in order to keep pseudo-first-order OH decay rates below ~1200 s^{-1} (a somewhat arbitrary choice made to permit the aquisition of suitably precise decay curves during convenient experimental run times). The limitations in precision and accuracy with which such low concentrations can be conveniently measured optically precluded our measuring H_2O_2 in the reactant flow entering and exiting the reaction cell over the full range of experimental concentrations. (For example, in the 200-nm region 10 mtorr of H_2O_2 is equivalent to little more than a 1% absorption over a 100-cm path length). Therefore the following alternative procedure was adopted.

Our experience with reaction cell and flow configurations in our recent nitric acid experiments [15] coupled with our previous observations on H_2O_2 heterogeneous decomposition [3] led us to believe that minimal H_2O_2 depletion would occur during the ~1 s transit time through the Pyrex reactor. This assumption was verified by absorption measurements for a range of flow rates (~50–200 cm^3/s) using H_2O_2 partial pressures in the 10–20-mtorr range. During the course of an experiment, then, the H_2O_2 was monitored in the bulk reaction mixtures (containing from ~0.2 to 0.6 torr H_2O_2 in 1 atm Ar) from which the reactant flows were metered. Such monitoring

was done by measuring the absorption of 213.9-nm radiation (using either a zinc or a deuterium lamp) in a 100-cm cell. For both lamps the radiation was isolated using an interference filter–monochromator combination. Absorptions of 10–50% were recorded, thereby permitting more precise computation of the H_2O_2 concentration in the reaction zone using an absorption cross section[2] of 3.10×10^{-19} cm^2. All sections of the apparatus which were exposed to the H_2O_2-containing mixtures were of Pyrex or Teflon fabrication. The 10-L bulb–100-cm absorption cell assembly was separated from the reaction cell by a very short section of tubing and a Teflon needle valve, resulting in minimal H_2O_2 decomposition during reaction cell traversal in the initial tests. The following factors thus defined our H_2O_2 concentration uncertainty: (1) flow control and reproducibility, (2) precision of the absorption measurements for the bulk mixtures, and (3) upper limit for H_2O_2 decomposition (set by the precision of measuring absorption in the 10–20-mtorr H_2O_2 mixtures). These composite uncertainties conservatively range from ~15% for the low end of our H_2O_2 concentration range to ~5% for the higher concentrations.

The Ar used in these experiments had a manufacturer's stated purity of 99.9999% and was used directly from the cylinder without further purification. Due to the use of water as our principal photolytic source of OH, we elected to obtain H_2O_2 from a 40% (by weight) H_2O_2–H_2O mixture. The constancy of the H_2O_2 vapor mole fraction could easily be verified by our absorption measurements. Distilled water was used after undergoing several freeze, pump, and thaw cycles.

Results

Due to our concern over the possible interference from secondary reactions, involving photolysis or reaction products, modeling calculations[3] were conducted on the reaction sequence

(5) $H_2O + h\nu \rightarrow H + OH$

(2) $H_2O_2 + h\nu \rightarrow OH + OH$

(1) $OH + H_2O_2 \rightarrow HO_2 + H_2O$

(4) $OH + HO_2 \rightarrow H_2O + O_2$

(6a) $H + H_2O_2 \rightarrow H_2O + OH$

(6b) $\rightarrow H_2 + HO_2$

(7a) $H + HO_2 \rightarrow OH + OH$

(7b) $\rightarrow H_2 + O_2$

(8) $OH + OH \rightarrow H_2O + O$

[2] This value is interpolated from the values recommended in [18].

[3] The modeling calculations were performed using an adaptation of a program package reported in [19].

(9) $$O + OH \rightarrow O_2 + H$$

(10) $$O + HO_2 \rightarrow OH + O_2$$

(3) $$HO_2 + HO_2 \rightarrow H_2O_2 + O_2$$

Rate constants were taken from the most recent evaluations.[4] Sources of measurement error can thus be broken into two categories: those reactions that consume additional OH [i.e., reactions (4), (8), and (9)] and those that regenerate OH [i.e., reactions (6), (7), and (10)], the extent of participation being determined by the initial OH (and/or H) concentration. Actinometric experiments conducted with the present flash lamp configuration indicated a light flux entering the reaction cell of approximately 6×10^{12} quanta/cm^2/flash in the 165–180-nm wavelength range for lamp operating pressures similar to those employed in this study. This value indicates that for the typical concentrations of H_2O and H_2O_2 used, the initial concentrations were $[OH]_0 \sim 1 \times 10^{11}$ cm^{-3} and $[H]_0 \lesssim 8 \times 10^{10}$ cm^{-3}. The modeling results showed that in this concentration range, as expected, secondary depletion of OH was totally negligible for more than a decadic decrease in OH. For example, when OH has decayed to 1×10^{10} cm^{-3} (i.e., $[HO_2] = 9 \times 10^{10}$ cm^{-3}), reaction (4) then contributes little more than 1% to the OH loss rate. Reaction (8), and thus reaction (9), are totally negligible for $[OH] < 3 \times 10^{12}$ cm^{-3}.

The secondary production of OH [primarily via reaction (7)] is somewhat more important and complex due to the initial presence of H atoms. However, the calculations indicated that for $[H]_0 \leq [OH]_0 \sim 10^{11}$ such regeneration of OH became important once product HO_2 had risen to approximately 5–10 times the remaining OH. Since two to three OH decay lifetimes are exceeded at such a point, the nonlinear least-squares fit to the decay curve is essentially unaltered. These modeling observations were confirmed by our experimental results, which indicated that (1) the calculated OH decay rates (for fixed $[H_2O_2]$) were unaffected by a fivefold variation in $[OH]_0$ (i.e., flash energy) about the 1×10^{11}-cm^{-3} value, and (2) within the statistical noise of the decay curves, no departure from exponential behavior was observed. Several such decay curves are presented in Figure 1.

In the absence of interferences from secondary reactions, then, the OH time history can be expressed as

$$\frac{-d[OH]}{dt} = k_1[OH][H_2O_2] + k_D[OH]$$

where k_D is a first-order loss rate of OH from our region of observation and is primarily diffusion controlled. Under such conditions, the first-order decay rate k^{1st} is related to k_1 by

$$k^{1st} = \tau_{1/e}{}^{-1} = k_1[H_2O_2] + k_D$$

[4] The primary source of rate constant recommendations was [20]. For those reactions not contained therein, we referred to [21].

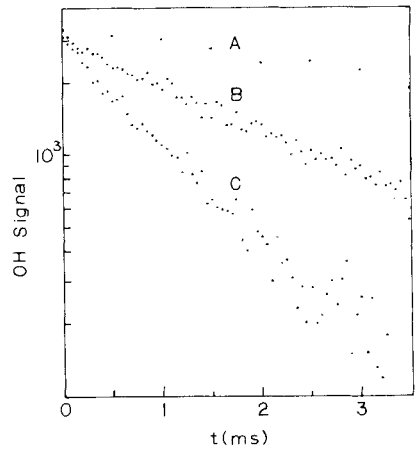

Figure 1. Typical OH decay curves. A—T = 296 K, 0.1 torr H_2O in 20 torr Ar; B—T = 278 K, 0.1 torr H_2O and 4.6 mtorr H_2O_2 in 20 torr Ar; C—T = 323 K, 0.1 torr H_2O and 14.5 mtorr H_2O_2 in 20 torr Ar.

where $\tau_{1/e}$ is the time interval required for [OH] to decay to e^{-1} of its initial value. Thus plots of k^{1st} versus $[H_2O_2]$ should be linear with a slope equal to k_1 at the temperature of the experiments (see Fig. 2). The slopes of these plots were calculated using an iterative solution of the "least-squares cubic" with errors in both x and y [22], thereby taking into account the uncertainties in both concentration and decay rate. The results from these analyses for the five different temperatures of this study are detailed in Table I. The intercepts from the fits (with the exception of 296 K) ranged from 140 to 200 s^{-1}, and within their 2σ statistical uncertainties were invarient with temperature. The intercept from the 296 K data was 105 s^{-1},

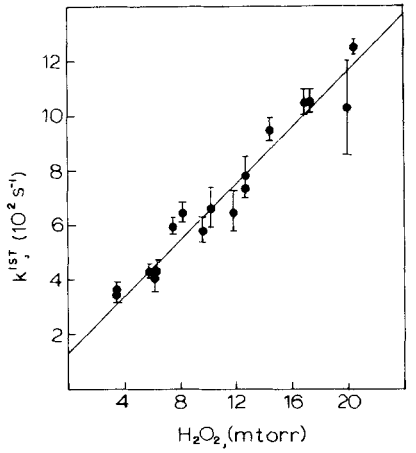

Figure 2. Plot of k^{1st} versus $[H_2O_2]$ at 323 K.

TABLE I. Summary of our measurements of k_1.

T (K)	$[H_2O_2]$ Range (mtorr)	$k_1 \times 10^{12}$ (cm^3/molecule s)
250	2.8–14.7	1.56 ± 0.21[a]
278	4.2–16.5	1.64 ± 0.25
296	0.0–20.9	1.79 ± 0.14
323	3.5–20.5	1.77 ± 0.25
370	3.7–15.1	1.90 ± 0.28

[a] Uncertainties shown are 2σ values from the "least-squares cubic" analysis detailed in the text.

the lower value being due to less restricted collimation on the viewing zone for those experiments. At each temperature the dynamic range of H_2O_2 concentration was chosen so that the highest decay rate measured was between 5 and 10 times faster than the limiting zero-concentration value (intercept).

The data from Table I are presented in an Arrhenius plot in Figure 3(A). The least-squares fit (using the same "least-squares cubic" solution referred to above) to the data is given by

$$k_1 = (2.93 \pm 0.49) \times 10^{-12} \exp[-(158 \pm 52)/T] \text{ cm}^3\text{/molecule s}$$

where the uncertainties are 2σ values from the analysis.

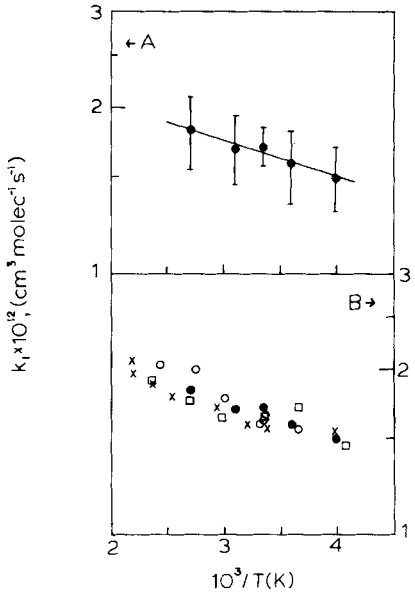

Figure 3. (A) Arrhenius plot of k_1 values from present work. Solid line—least-squares fit. (B) Arrhenius plot of k_1 values from the most recent studies: ●—this work; ○—Wine et al. [14]; ×—Sridharan et al. [13]; □—Keyser [12].

Figure 3(B) shows a composite Arrhenius plot of all the data from the four most recent temperature-dependent investigations. For the purposes of comparison, all the k_1 values have been recalculated using the absorption cross-section data employed in the present work [18]. This results in a lowering of the Sridharan et al. [13] data by ~4%, no change in the Keyser [12] data, and an increase of ~8% in the results of Wine et al. [14]. A linear least-squares analysis of this revised data set yields

$$k_1 = (2.91 \pm 0.30) \times 10^{-12} \exp[-(161 \pm 32)/T] \text{ cm}^3/\text{molecule s}$$

an expression which is virtually indistinguishable from the fit to our data alone and is very similar to that now recommended for use in atmospheric modeling calculations.

Discussion

While the reported E/R values from the four most recent studies (ours included) range from 126 to 260 K, the individual rate constant spread at any one temperature is less than 20% in the temperature region of measurement. Such agreement is certainly suggestive of the greater accuracy of these measurements relative to the earlier investigations. The factor of 2 and greater differences from these latter studies have been ascribed qualitatively by Keyser [12] and more quantitatively by Sridharan et al. [13] to secondary chemistry. Since we found it necessary to perform modeling calculations to evaluate uncertainties in our own experiments, we extended these computations to the experimental conditions of the studies of Hack et al. [7], Harris and Pitts [8], and Greiner [6]. The results of the exercise are particularly revealing with respect to the coupling among various secondary reactions in this chemical system: they demonstrate significant problems in all three of the early absolute measurements, while confirming the validity of the present determinations. For this reason we present a summary of these calculations here.

The discharge-flow electron spin resonance experiments of Hack et al. [7] utilized OH concentrations $\leq 3 \times 10^{13}$ to suppress such reactions as (8) and (9). They incorrectly assumed, however, that the rapidity of reaction (4) relative to reaction (1) would result in a full stoichiometry of 2 for OH depletion in this system. Modeling calculations of their room temperature experiments are presented in Figure 4. Curve A was generated using $[OH]_0 = 8 \times 10^{12}$ cm^{-3} and $[H_2O_2] = 1 \times 10^{14}$ cm^{-3} and included reactions (1), (3), (4), and (6)–(10). Curve C is the expected decay at these concentrations using only reaction (1) (i.e., stoichiometry = 1); while curve D assumes a stoichiometry of 2. As can be clearly seen, the OH decay lies approximately midway between these extremes. When reaction (11) is included in the model, curve B is generated:

(11) $$HO_2 + NO \rightarrow OH + NO_2$$

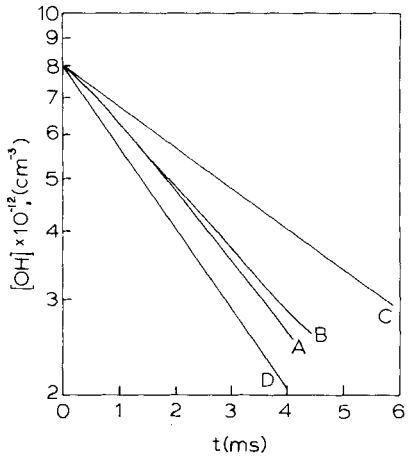

Figure 4. Computer simulation of the experiments of Hack et al. [7] with $[OH]_0 = 8 \times 10^{12}$ cm^{-3} and $[H_2O_2] = 1 \times 10^{14}$ cm^{-3}. A—Model uses reactions (1), (3), (4), and (6)–(10); B—same as A, but includes reaction (11) with $[NO] = [OH]_0$; C—OH decay due to reaction (1) alone with $k_1 = 1.7 \times 10^{-12}$ cm^3/molecule s; D—OH decay due to reaction (1), but assuming a factor of 2 stoichiometry.

NO was present in the experiments of Hack et al. [7] as a product of the H atom/NO_2 titration used to produce OH and thus $[NO] = [OH]_0$. Inclusion of this reaction leads to a noticeable production of OH at long reaction times when compared with curve A, thereby lessening somewhat the effect of reaction (4). We conclude that an average stoichiometry of ~1.6 better typified these experiments than the factor of 2 that was assumed. It should be emphasized, however, that these results depend on accurate knowledge of $[OH]_0$ and [NO]. Correcting for an overestimation of $[OH]_0$ and/or $[H_2O_2]$ coupled with an underestimation of [NO] could shift curve A even closer to curve C.

The FPRF study of Harris and Pitts [8] is very similar to our own,with the exception that these authors produce H atoms from the photolysis of both H_2O and H_2O_2 at wavelengths significantly shorter than our 165-nm photolysis cutoff. While these authors do not report a value of $[OH]_0$, in earlier studies [23] they estimate the concentration as ~10^{11} cm^{-3}. We thus performed the modeling calculations for 10^{11} cm$^{-3} \leq [OH]_0 \leq 10^{12}$ cm^{-3}; $\frac{1}{3} \leq [H]_0/[OH]_0 \leq 1$; and $[H_2O_2] = 3 \times 10^{14}$ cm^{-3}. To the reactions listed in the previous model were added diffusion of the radical species from the viewing zone (~25 s^{-1} as measured by the authors). The results of these computations appear in Figure 5. Curves A and B utilize $[OH]_0 = 1 \times 10^{11}$ cm^{-3} with $[H]_0/[OH]_0 = \frac{1}{3}$ and 1, respectively. As can be seen, the higher the $[H]_0/[OH]_0$ ratio, the greater the secondary production of OH at long reaction times. Nevertheless, even for curve B there is little error over the first decadic decrease in OH when compared with curve E (offset for clar-

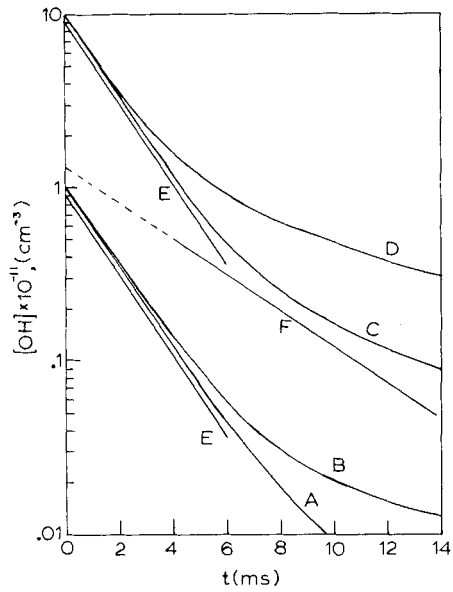

Figure 5. Computer simulation of experiments of Harris and Pitts [8] using reactions (1), (3), (4), and (6)–(10) plus diffusion. $[H_2O_2] = 3 \times 10^{14}$ cm^{-3}. A—$[OH]_0 = 1 \times 10^{11}$ cm^{-1}, $[H]/[OH]_0 = \frac{1}{3}$; B—$[OH]_0 = 1 \times 10^{11}$ cm^{-3}, $[H]/[OH]_0 = 1$; C—$[OH]_0 = 1 \times 10^{12}$ cm^{-3}, $[H]/[OH]_0 = \frac{1}{3}$; D—$[OH]_0 = 1 \times 10^{12}$ cm^{-3}, $[H]/[OH]_0 = 1$; E—OH decay due to reaction (1) alone with $k_1 = 1.7 \times 10^{-12}$ cm^3/molecule s, offset for clarity; F—OH decay due to reaction (1) alone with $k_1 = 6.8 \times 10^{-13}$ cm^3/molecule s.

ity), whose slope corresponds to OH decay in the total absence of secondary reactions. More specifically, a nonlinear least-squares fitting to an exponential function is prejudiced toward fitting the early time (higher fluorescence signal) values, while in a semilogarithmic presentation (shown here) the reverse is true. Thus little if any error in the decay curve fits should have been realized for radical concentrations below 10^{11}. When $[OH]_0$ is raised to 10^{12} cm^{-3}, curves C and D are generated. It is quite evident that when secondary generation of OH is large enough to compete with the normal decay, rather severe digressions from exponential behavior occur, and a force fit to a simple exponential function would be much less steep than curve E. Curve F is presented to show an OH decay plot with a k_1 value equal to that reported by Harris and Pitts. Such a value could be obtained if the fitting emphasized the OH time profile for $t \gtrsim 1$ ms. Reasonably precise data, however, should have revealed the nonexponential behavior in the OH decay curves under such conditions. The authors did observe mixed kinetic decays at high radical concentrations, but confined their data analysis to curves showing strictly first-order behavior. It is possible that the poorer signal levels at the low concentrations masked the

complexity of the decay. Such a problem coupled with any significant depletion of H_2O_2 could produce the results reported.

The computer simulation of Greiner's experiments [6] indicate that the room temperature data in particular were misinterpreted. The experiments, while simplified by the absence of a significant initial H atom concentration, have an added complexity generated by OH + OH disproportionation [reaction (8)] at the very high OH concentrations used. This causes a slightly *delayed* buildup of H and O atoms, which react to regenerate OH at a rate competitive with OH decay at the longer reaction times. Curve A in Figure 6 represents OH decay in the presence of ~1 torr of H_2O_2 using the full mechanism described earlier. As can be seen, the early time profile for OH is slightly steeper than predicted by the occurrence of reaction (1) alone (curve B), while at times around 100 μs the actual decay is noticeably slower. It was this second portion of the decay curve that Greiner ascribed to reaction (1) and used to report a value which corresponds to curve C. Our calculations show that the inflection point in curve A depends strongly on the value of $[OH]_0$. Thus the fact that curve C better represents the limiting OH decay rate in the 100–200-μs region than in the 70–130-μs range over which Greiner performed his analysis is not a serious disparity. A depletion of H_2O_2 (above that assumed by the author) could also have contributed to the error in k_1. Greiner's higher temperature data essentially made use of the initial slopes, and therefore are only slightly higher than would be predicted by the present work at those temperatures.

The two classical photochemical studies [9,10] for k_1 yield results dif-

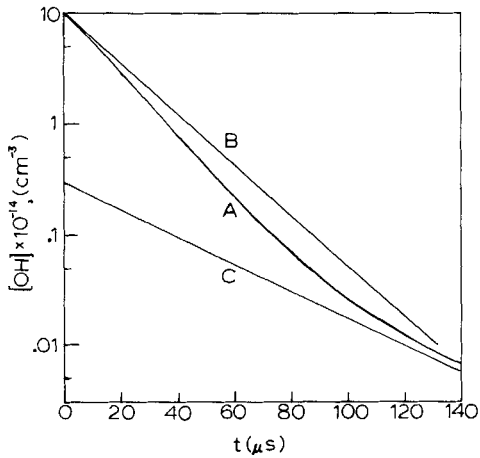

Figure 6. Computer simulation of experiments of Greiner [6] using reactions (1), (3), (4), and (6)–(10) with $[OH]_0 = 1 \times 10^{15}$ cm^{-3} and $[H_2O_2] = 3 \times 10^{16}$ cm^{-3}. A—Full model results; B—OH decay due to reaction (1) alone with $k_1 = 1.7 \times 10^{-12}$ cm^3/molecule s; C—OH decay corresponding to $k_1 = 9.4 \times 10^{-13}$ cm^3/molecule s.

fering by a factor of 2 from each other and are significantly lower than the present measurements. As these determinations use the OH + CO reaction as a reference, they may suffer complications due to its reported complex dependence on pressure and O_2 concentrations [24]. Thus it is very difficult to assess the uncertainties associated with these early relative measurements.

It appears that our understanding of the OH + H_2O_2 reaction system has progressed markedly over the past two years to a point where the four most recent studies yield a very consistent representation of the T dependence for k_1. In addition we can offer some rather quantitative appraisals of secondary complications in the earlier investigations, which resolve to a large part the differences in the rate constants reported. This computational exercise demonstrates the utility and (in some cases) necessity of combining kinetic measurements with modeling calculations based on known radical concentrations. Such computer simulations enable one to perform data analyses incorporating demonstrated rather than assumed kinetic behavior. Due to the difficulties in measuring k_1 and the limitations in the temperature range over which precise measurements of $[H_2O_2]$ can be made, the use of an Arrhenius expression for k_1 (based on all four most recent studies) for atmospheric modeling applications is recommended.

$$k_1 = (2.91 \pm 0.31) \times 10^{-12} \exp[-(161 \pm 32)/T] \text{ cm}^3/\text{molecule s}$$

Extrapolation of this equation outside of the combined temperature extremes of these studies (245 K $\leq T \leq$ 460 K) should be done with caution. The conclusions reached by Keyser [12] and Sridharan et al. [13] concerning the effect of their k_1 measurements on HO_x profiles and H_2O_2 atmospheric loss are supported by the results reported herein. Similarly, their discussion of the effects of the new k_1 values on other laboratory studies involving HO_2 need not be duplicated here.

Acknowledgment

This work was supported in part by the Fluorocarbon Research Program of the Chemical Manufacturers Association. The authors would like to thank Dr. R. F. Hampson (NBS) for his helpful comments during the preparation of this manuscript.

Bibliography

[1] C. J. Howard, Proc. NATO Advanced Study Institute on Atmospheric Ozone, Algarve, Portugal, 1979, FAA-EE-80-20, pp. 409–427.
[2] R. A. Cox and J. P. Burrows, *J. Phys. Chem.*, **83,** 2560 (1979).
[3] M. J. Kurylo, O. Klais, and A. H. Laufer, *J. Phys. Chem.*, **85,** 3674 (1981).
[4] W. B. DeMore, *J. Phys. Chem.*, **86,** 121 (1982).
[5] NASA Panel for Data Evaluation, Evaluation no. 4, J. P. L. Publ. 81-3, Jan. 1981.
[6] N. R. Greiner, *J. Phys. Chem.*, **72,** 406 (1968).

[7] W. Hack, K. Hoyermann, and H. Gg. Wagner, *Int. J. Chem. Kinet.*, **1,** 329 (1975).
[8] G. W. Harris and J. N. Pitts, *J. Chem. Phys.*, **70,** 2581 (1979).
[9] J. E. Meagher and J. Heicklen, *J. Photochem.*, **3,** 455 (1975).
[10] R. A. Gorse and D. H. Volman, *J. Photochem.*, **1,** 1 (1972).
[11] NASA Panel for Data Evaluation, Evaluation no. 2, J. P. L. Publ. 79–27, Apr. 1979.
[12] L. F. Keyser, *J. Phys. Chem.*, **84,** 1659 (1980).
[13] U. C. Sridharan, B. Reimann, and F. Kaufman, *J. Chem. Phys.*, **73,** 1286 (1980).
[14] P. H. Wine, D. H. Semmes, and A. R. Ravishankara, *J. Chem. Phys.*, **75,** 4390 (1981).
[15] M. J. Kurylo, K. D. Cornett, and J. L. Murphy, *J. Geophys. Res.*, **87,** 3081 (1982).
[16] M. J. Kurylo, *Chem. Phys. Lett.*, **58,** 233 (1978).
[17] O. Klais, P. C. Anderson, and M. J. Kurylo, *Int. J. Chem. Kinet.*, **12,** 469 (1980).
[18] NASA Panel for Data Evaluation, Evaluation no. 5, JPL Publ. 82-57, July 1982.
[19] R. L. Brown, "A Computer Program for Solving Systems of Chemical Rate Equations," NBSIR 76-1055, National Bureau of Standards, Washington, DC, 1976.
[20] R. D. Hudson, E. I. Reed, and R. D. Bojkov, "The Stratosphere 1981: Theory and Measurement," Appendix 1, WMO/NASA 1981.
[21] D. L. Baulch, R. A. Cox, R. F. Hampson, J. A. Kerr, J. Troe, and R. T. Watson, *J. Phys. Chem. Ref. Data*, **9,** 295 (1980).
[22] D. York, *Can. J. Phys.*, **44,** 1079 (1966).
[23] R. Atkinson, D. A. Hansen, and J. N. Pitts, *J. Chem. Phys.*, **63,** 1703 (1975).
[24] H. W. Biermann, C. Zetzsch, and F. Stuhl, *Berg. Bunsenges. Phys. Chem.*, **82,** 633 (1978).

Received March 29,1982
Accepted June 11, 1982